**Molecular Engineering of Conjugated Polymers for Efficient Hole Transport and Defect Passivation in Perovskite Solar Cells**

Feilong Cai[1,2], Jinlong Cai[1,2], Liyan Yang[1,2], Wei Li[1,2], Robert S. Gurney[1,2], Hunan Yi[3], Ahmed Iraqi[3], Dan Liu[1,2], Tao Wang[1,2]*

[1]State Key Laboratory of Silicate Materials for Architectures, Wuhan University of Technology, Wuhan, 430070, China

[2]School of Materials Science and Engineering, Wuhan University of Technology, Wuhan, 430070, China * E-mail: twang@whut.edu.cn

[3]Department of Chemistry, University of Sheffield, Sheffield, S3 7HF, UK

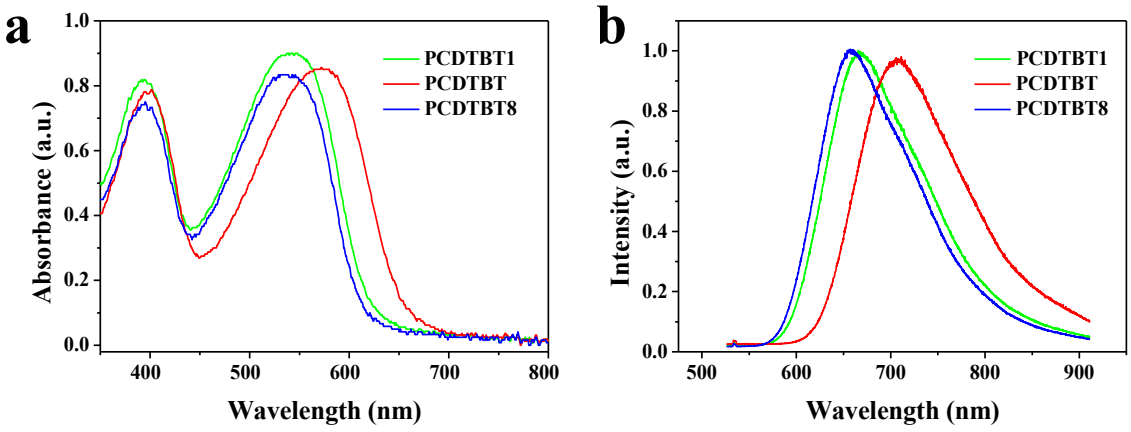


**Figure S1.** Optical properties of three conjugated polymers. (a) Absorption and (b) photoluminescence (PL) spectra of ITO/PCDTBT1, ITO/PCDTBT and ITO/PCDTBT8.

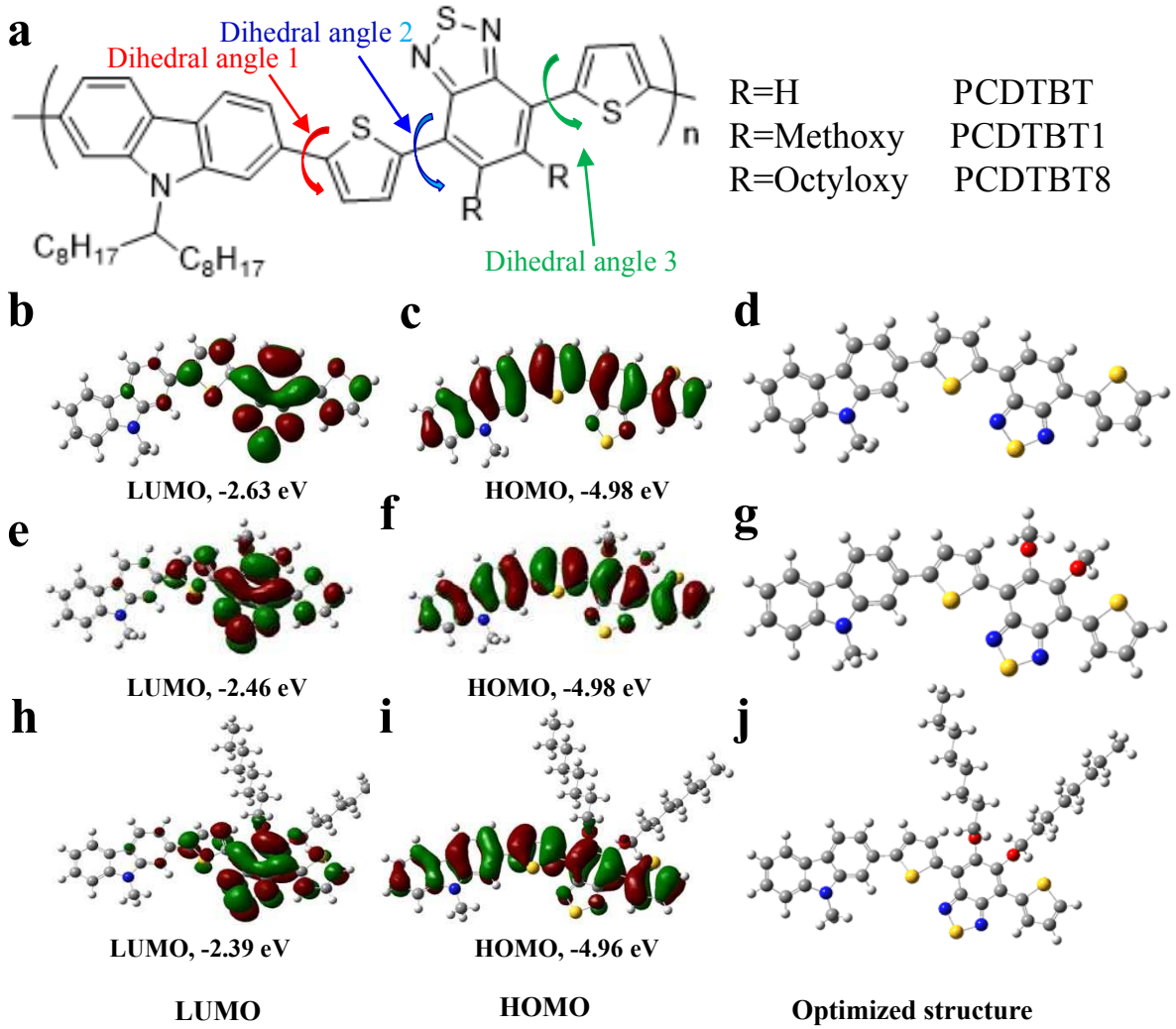


**Figure S2.** Geometry-optimized structures and frontier molecular orbitals of three conjugated polymers. (a) Chemical structures of conjugated polymers with three dihedral angles. (b-d), (e-g), (h-j) are the electron density distributions of frontier molecular orbitals obtained from DFT caculations and their geometry-optimized structures of the PCDTBT, PCDTBT1 and PCDTBT8, respectively.

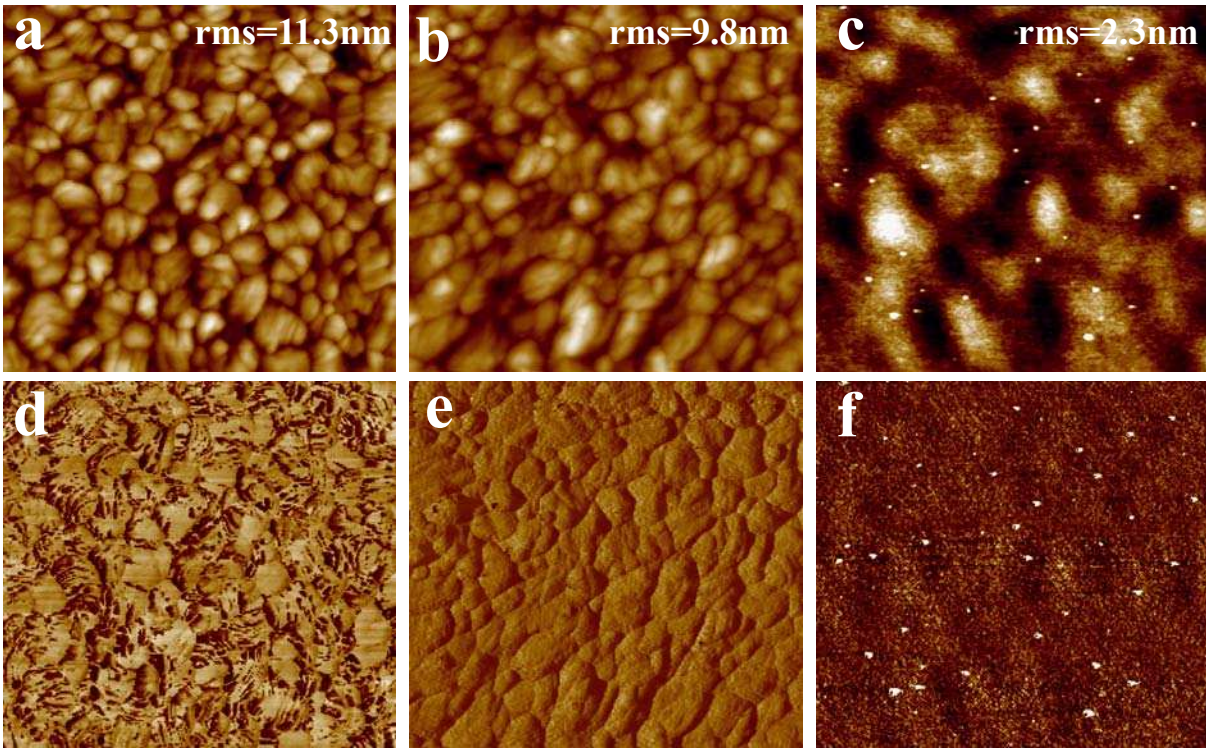


**Figure S3.** Surface morphology characterization. SPM surface height images from films made of (a) perovskite, (b) perovskite/PCDTBT1 (c) perovskite/Spiro-OMeTAD and (d-f) are the corresponding phase images respectively. Image size is 5 μm ×5 μm.

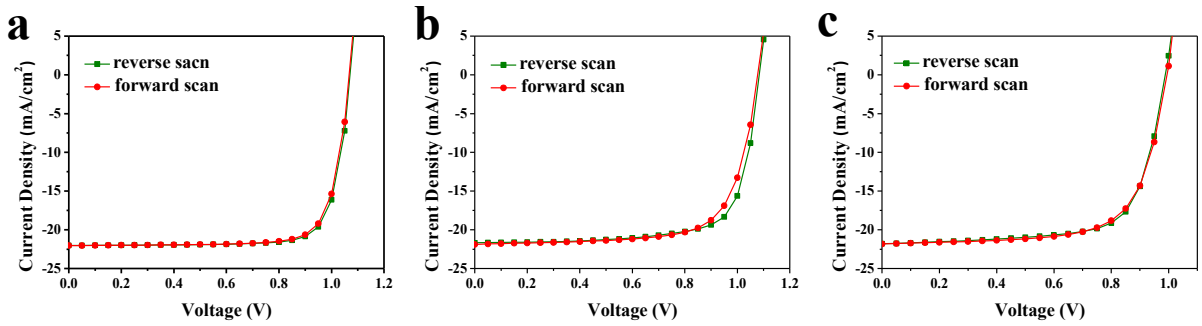


**Figure S4.** Hysteresis of devices having different HTMs. *J-V* curves of devices using (a) PCDTBT1, (b) PCDTBT and (c) PCDTBT8 as HTMs.

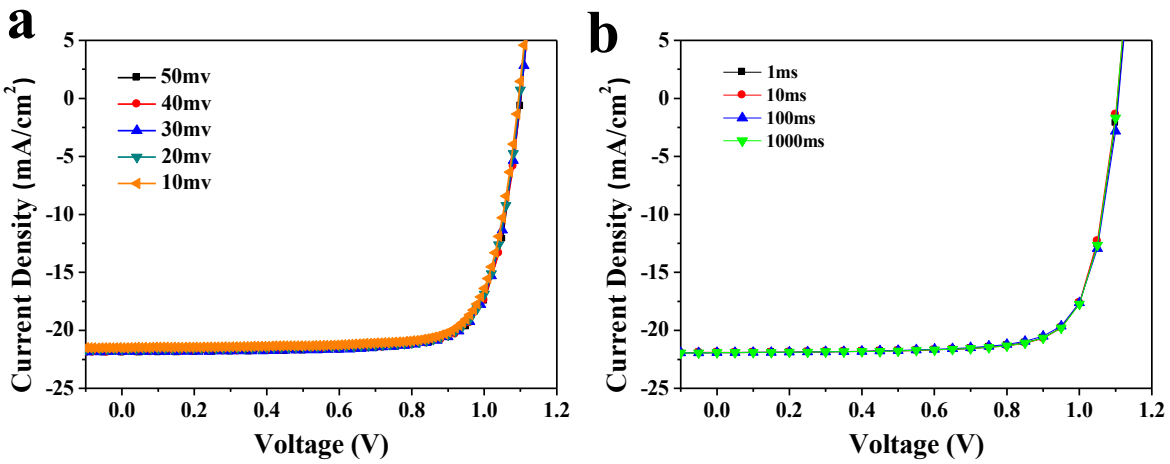


**Figure S5.** Photovoltaic performance measured under different scan rates and delay times. *J-V* curves of the same device measured with different (a) scan delay times and (b) voltage step sizes.

**Table S1.** Device metrics parameters of perovskite solar cells employing different HTMs. The active area is 4 mm$^2$ for each device.

| HTMs | Scan direction | $V_{oc}$(V) | FF | $J_{sc}$ (mA cm$^{-2}$) | PCE$_{ave}$ (PCE$_{max}$) |
|---|---|---|---|---|---|
| PCDTBT | RS | 1.04±0.01 | 71.64±1.15 | -21.52±0.24 | 16.13±0.39(16.8) |
| | FS | 1.04±0.01 | 71.32±1.35 | -21.34±0.36 | 16.02±0.34(16.7) |
| PCDTBT1 | RS | 1.09±0.01 | 77.12±1.26 | -21.65±0.45 | 18.42±0.35(18.9) |
| | FS | 1.09±0.01 | 76.98±1.12 | -21.52±0.38 | 18.32±0.29(18.6) |
| PCDTBT8 | RS | 1.01±0.01 | 66.91±1.02 | -21.12±0.39 | 14.41±0.37(15.1) |
| | FS | 1.01±0.01 | 66.25±0.98 | -21.06±0.46 | 14.36±0.46(14.8) |

$V_{oc}$, open circuit voltage; FF, fill factor; $J_{sc}$, short-circuit current density; PCE, power conversion efficiency.

Average performance parameters and their S.D. were obtained based on 20 cells for each set.

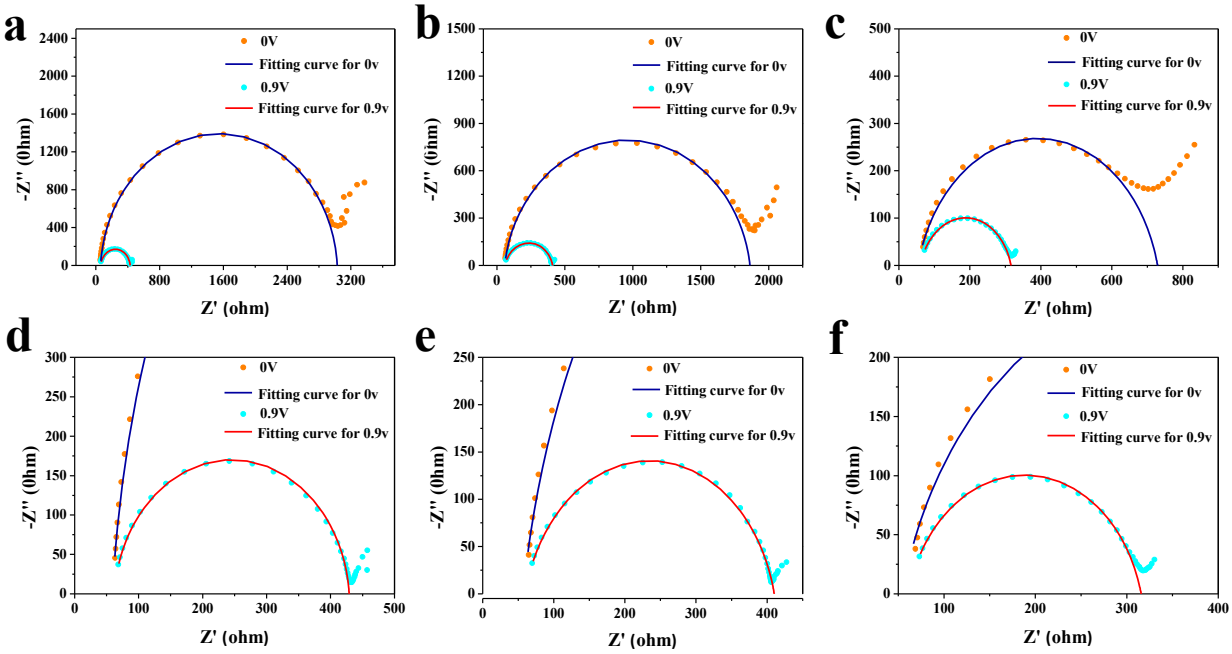


**Figure S6.** Nyquist plots of devices with different HTMs. (a), (b) and (c) correspond to EIS measurements under 1-sun illumination incorporating PCDTBT1, PCDTBT and PCDTBT8 as the HTMs, respectively. (d), (e) and (f) are zoomed-in on the low impedance region for (a), (b) and (c) respectively to show the results at 0.9 V applied bias clearly.

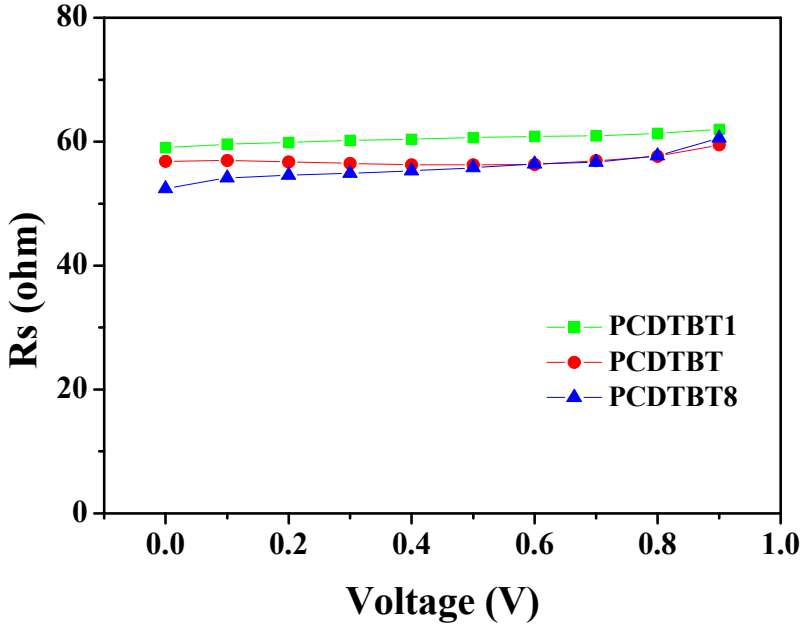


**Figure S7.** The *Rs* values of devices empolying different HTMs obtained from fitting the

results through the equivalent circuit.

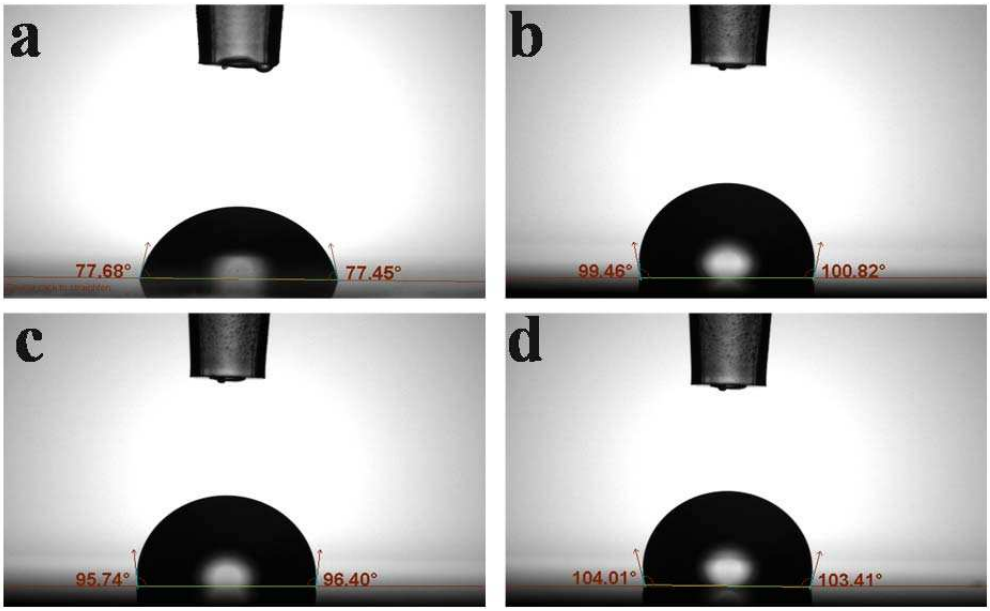


**Figure S8.** Surface hydrophobicity analysis. The water contact angle images of (a) spiro-OMeTAD, (b) PCDTBT, (c) PCDTBT1 and (d) PCDTBT8.

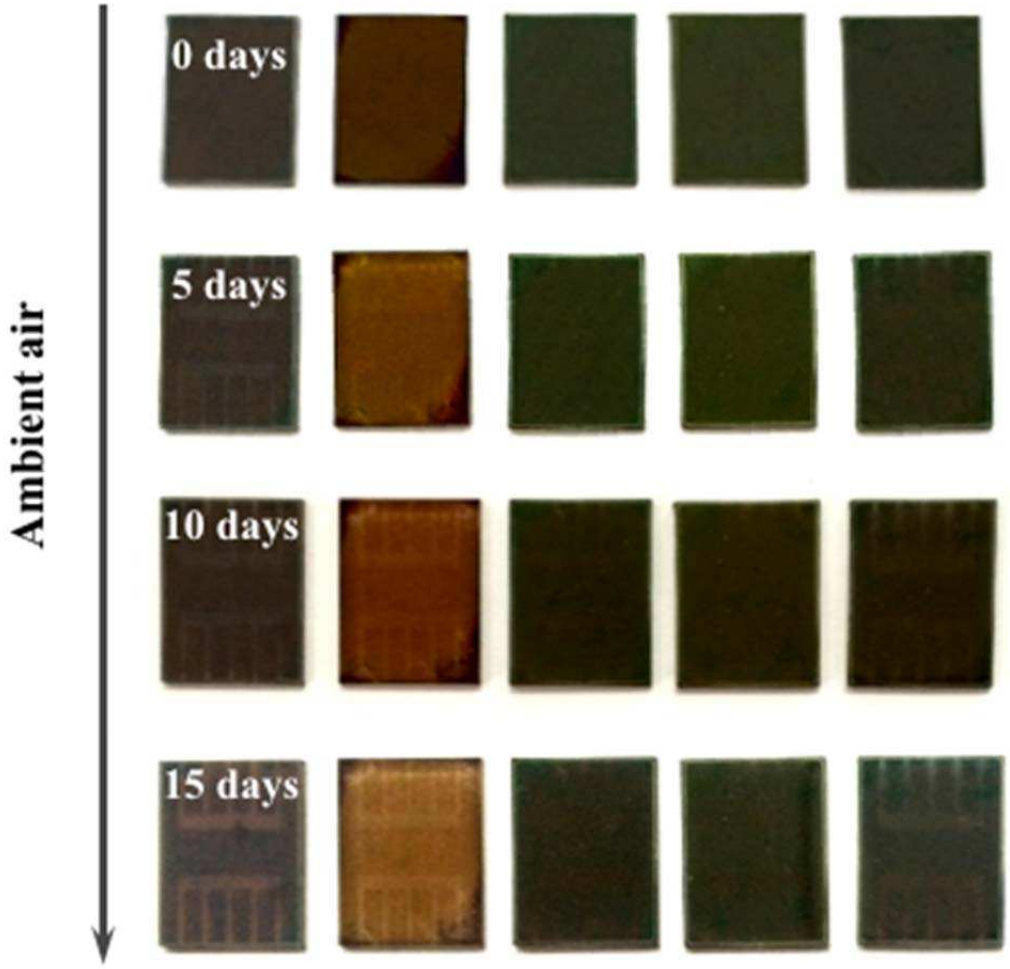


**Figure S9.** Stability test of perovskite devices. Images of perovskite, perovskite/ spiro-OMeTAD, perovskite/PCDTBT1, perovskite/PCDTBT and perovskite/PCDTBT8 (from left to right, respectively) films under different durations of exposure in ambient (40~70 RH%).